1. Introduction

The Earth's climate responds to long-term (10^4 to 10^5 years) variations in the Earth's orbital parameters, commonly summarised in the *Milankovitch theory* [e.g. Hays et al., 1976; Berger, 1978], and these variations result in warm and cold periods on that time scale. Periods with a long-term decrease in the surface temperature on the Earth and a drop by more than 10°C result in an expansion of the continental ice sheets, polar ice sheets and mountain glaciers. These colder phases with advancing ice sheets are called *glacials*. Warmer phases with retreating ice sheets are termed *interglacials*. The entire period is commonly referred to as *ice age cycle*, and the *ice age* comprises several cycles. Today, we live in an interglacial of an ice age.

Since the beginning of the Quaternary 2.59 million years ago, the Earth has experienced several cycles of glaciation (cyclicity of about 120,000 years) with ice sheets advancing and retreating in North America, Northern Eurasia, Greenland and Antarctica. In Northern Germany, the cold periods were known as the Elster glacial, the Saale glacial and the Weichsel glacial. The last time the Earth was covered by large ice sheets ca. 22,000 years ago, an era referred to as the *Last Glacial Maximum* (LGM). The last remnants of the Late Pleistocene ice sheets vanished around 6000 years ago.

Fig. 1.1 shows the additional ice covering the Northern Hemisphere during the last glacial cycle. North America experienced the largest ice-sheet growth with up to 3400 m thickness during the LGM. The Greenland Ice Sheet was around 500 m thicker than today (3000 m) and in Fennoscandia the ice height reached around 1700 m in the centre. Furthermore, smaller ice sheets covered the British Isles and the Barents Sea. In contrast to the retreat shown in Fig. 1.1, most of the ice masses of the Greenland Ice Sheet and the Antarctic Ice Sheet on the Southern Hemisphere have survived until the interglacial period, today representing the two major ice sheets. The former major ice sheets occupied $\sim$30% of the land area at the LGM, compared to $\sim$10% today.

The spatial and temporal distribution of the ice sheets is constrained by glacial moraines, glacigenic sediments, and glacial striations. From field evidence such as moraines and glacial erratics the extent of the ice sheets at a certain time is reconstructed, and the glacial striations show the direction of the ice flow. Finally, the $\delta^{18}O$ record and numerical models are needed to get the information about the timing, the height and the flow of the ice sheets, which are necessary for the construction of a time-dependent and three-dimensional (3D) ice model. In this work, the global ice model **RSES** for the Late Pleistocene glacial history will be used, compiled by Kurt Lambeck at the **R**esearch **S**chool of **E**arth **S**ciences, Canberra, Australia.

During the LGM, 5.5% of the world's water was bound in ice, as opposed to 1.7% today [Williams et al., 1998]. The transfer of water from the oceans to the expanding ice sheets resulted in a global sea level fall by an average of up to 130 m [Fairbanks, 1989; Fleming et al., 1998; Yokoyama et al., 2000]. Fig. 1.2 summarises the contributions of the major glaciated regions to the total amount of the sea-level fall as calculated with the ice model RSES. It can be seen that more than a half of the transferred water was bound in the ice sheet of North America, around one third in the enlarged Antarctic Ice Sheet, and "only" one seventh in the Fennoscandian region.

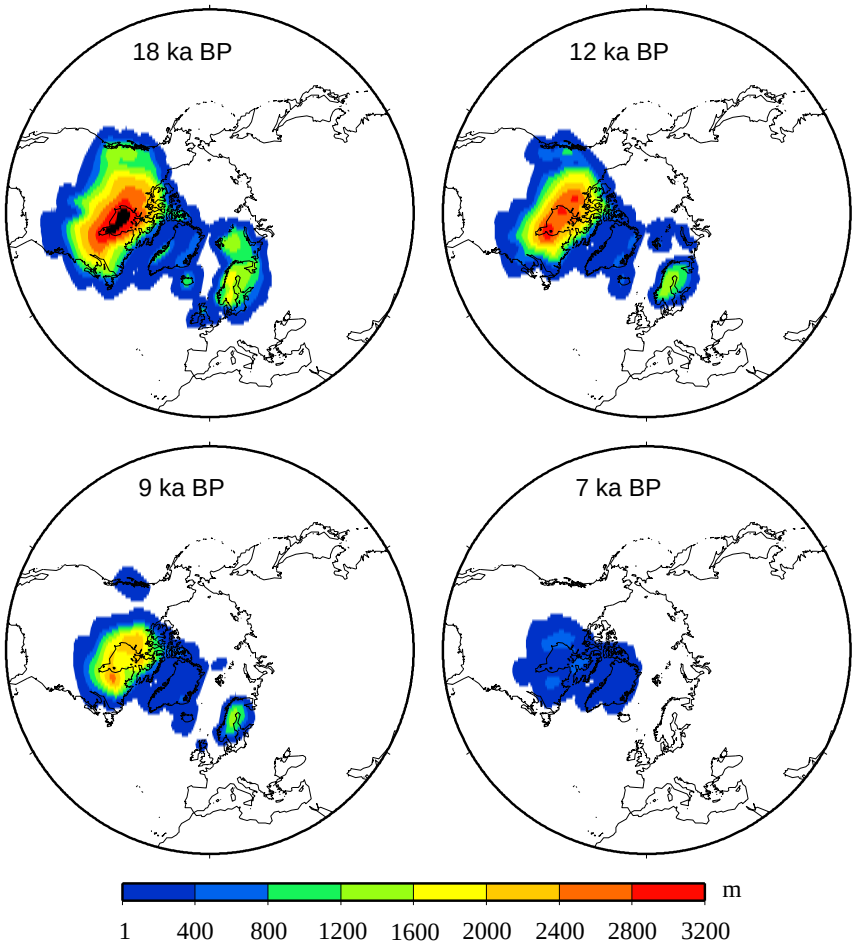

Figure 1.1: The additional ice on the Northern Hemisphere at four times during the last ice age.

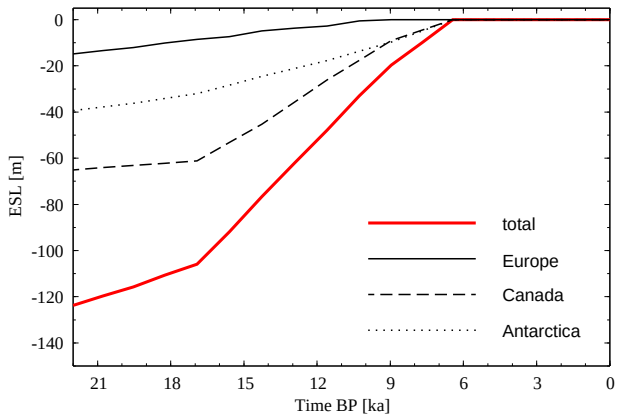

Figure 1.2: Estimated sea-level change induced by the ice sheets of the last ice age, calculated with the global ice model RSES [from Kaufmann, 2004].

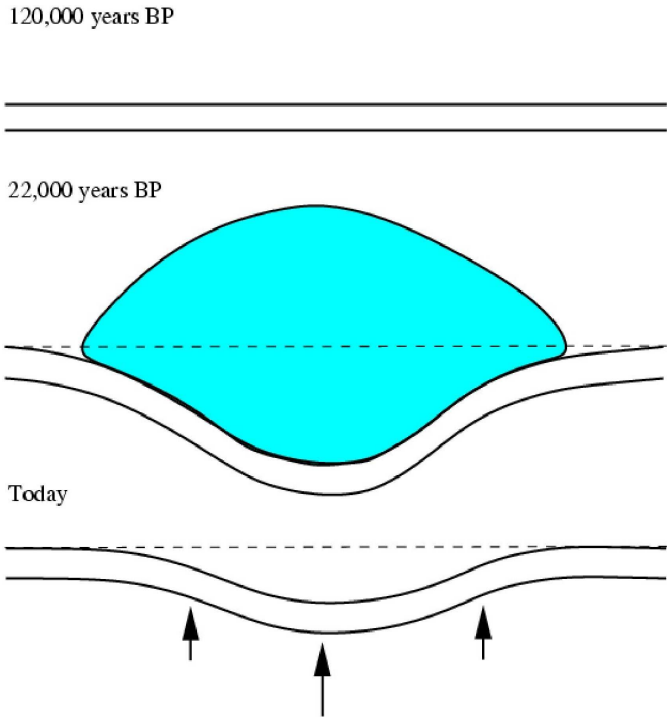

Figure 1.3: Sketch of the rebound principle [modified from Kaufmann, 2004].

Due to the water-mass transfer between the ice sheets and the ocean, the Earth's crust and mantle were deformed by the changing weight of the ice sheets on land and the water load in the oceans. This process, termed *glacial isostatic adjustment* (GIA), is sketched in Fig. 1.3: 125,000 years ago, during the Last Interglacial, the Earth's surface was free of additional ice and the crust and the mantle have (almost) relaxed after the former glaciation. No deformation is observed. During the build-up of the ice sheets until the LGM at 22,000 years BP, the surface was depressed by several hundreds of metres. The enormous weight of this ice caused the crust to sink into the fluid mantle. During the melting phase, the surface rebounded due to the buoyancy of the displaced material relative to the mantle, but not to its initial state. This lag is due to the time-dependent viscoelastic relaxation of the Earth's mantle with its fairly high viscosity. The GIA is still going on and thus observable today. It is documented by numerous observations all around the world. In Fennoscandia and northwestern (NW) Europe, where the large Weichselian Ice Sheet complex was located during the last glacial cycle, the GIA process was early recognised in numerous field observations [see Ekman, 1991, for a review]. Here, the scientific record of the crustal response is documented in various observations such as (i) palaeo-strandlines (relative sea levels, RSL), (ii) tide gauges, (iii) shoreline tilting, (iv) present-day crustal deformations monitored by GPS observations, and (v) present-day changes in the gravity field seen by satellite missions and field campaigns. Together with the knowledge of the ice-sheet retreat since the LGM, this large set of different observations, both in space and time, provides a detailed picture of the past and ongoing deformation. The database allows, amongst other things, to construct a detailed model of sea-level change induced by the mass redistribution between ice sheets and the ocean.

From the five observation types mentioned above, the last three methods (tilt, GPS, gravity) comprise short time periods in the decadal range, which is very short compared to the relaxation time. With these

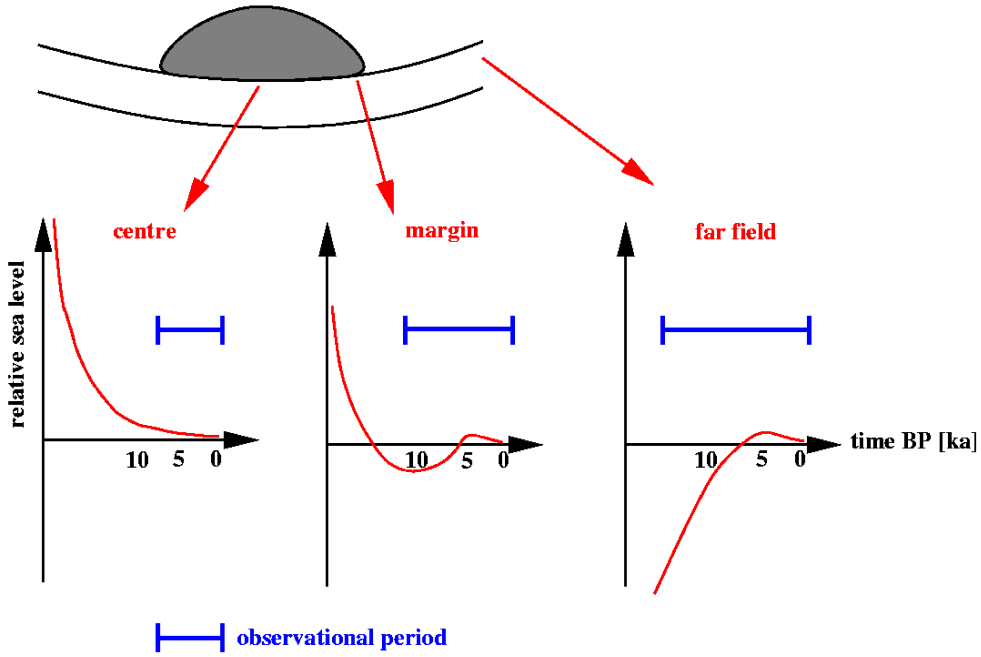

Figure 1.4: Anatomy of sea-level records in distance to the ice sheet [modified from Kaufmann, 2004].

methods the present-day GIA is observed. The tide gauge records are available from some selected stations since ca. 300 years, comprising a longer time period than the three other methods, but still short compared to the relaxation time. The longest time period is covered by RSL data, where two main parts contribute to: (i) the isostatic contribution resulting from the deformation of the solid surface by ice loading/unloading, (ii) the eustatic contribution due to the change in the sea level as a consequence of mass conservation. Hence, the RSL curve at a particular location varies with distance to the former ice sheet. Fig. 1.4 summarises these effects: In the centre of the ice sheet, the isostatic component is largest and the uplift has taken place in two distinct stages: The initial uplift was rapid and took place as the ice was being unloaded. Once the deglaciation was complete, the uplift was slower and decreased exponentially after that. The observational period starts when the last ice is melted. At the margin of the ice sheet the isostatic contribution is smaller than in the centre and the eustatic contribution becomes more important. Thus, until 10,000 years BP a sea-level fall is observed to a point below the present-day sea level. Then the eustatic contribution dominates until today. As the ice vanishes earlier at the margin, the observational period also starts earlier. In the far field only the eustatic part contributes to the RSL, which allows an observational period over the whole deglaciation. It is possible that the sea level rises to points higher the sea level today (Holocene highstand). Due to the increasing water load, the surface of the ocean basin and/or the continental shelf is depressed again (5000 years BP). Today, typical uplift rates in the centre of formerly glaciated areas are in the order of 10 mm/yr [see Johansson et al., 2002] and typical rates of sea-level rise are in the order of 1.5 mm/yr [see Töppe, 1992, 1995].

Fennoscandia and NW Europe turned out to be key regions of investigations to GIA, due to a large number of available observation data. Some examples for sea-level data in these regions are presented in Fig. 1.5. Ångermanaelven is located in the centre of the former Fennoscandian Ice Sheet and thus experiences a monotonic land uplift. The earliest data have an age of ca. 10,000 years BP, indicating the time when this location became ice free. In contrast to Ångermanaelven, Zeeland shows the typical

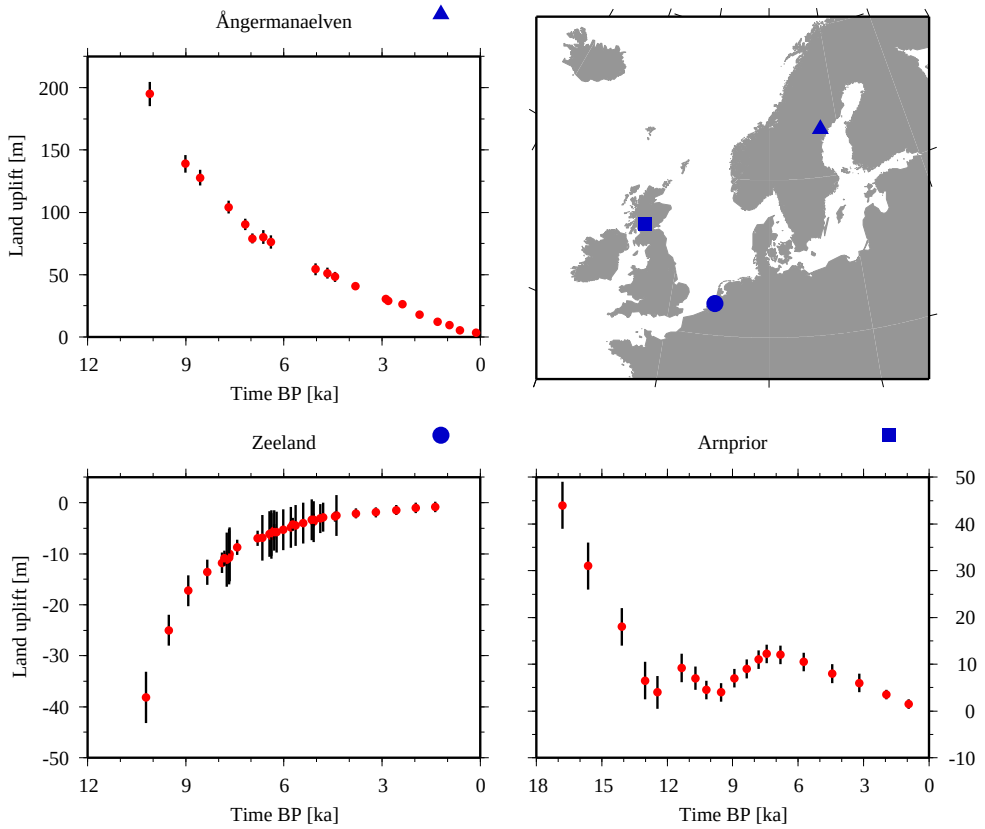

Figure 1.5: Examples of sea-level data (red dots with error bars) in Europe showing the different types of RSL curves.

eustatic sea-level curve. Here, the data record also begins around 10,000 years BP. This is due to the fact that the North Sea was above sea level during the last ice age. The first observation mark holds the time when the first water left a trace in near distance to the present-day coastline and the sea level rose steadily due to the melt-water impact. The last example from the location of Arnprior includes both the isostatic and the eustatic component. Furthermore, this data set envelopes a long time period, starting at 17,000 years BP. The first part until 11,000 years BP includes the uplift phase after the melting of the British Isles Ice Sheet and the eustatic contribution. After 11,000 years BP, one can see again a short dominating isostatic part for around 2000 years, which is induced by a short readvance (Loch Lomond readvance) of the British Ice Sheet. Then the eustatic part dominates.

In addition to the RSL data set, the GPS observations from the BIFROST project [Johansson et al., 2002, Fig. 1.6] are often used in investigations of the rebound in Fennoscandia. These 44 stations monitor the ongoing crustal deformation of the Netherlands and the United Kingdom in the Southwest to Sweden and Finland in the Northeast, and thus provide the present-day vertical and horizontal crustal motion in that region. The data show a broad ellipsoidal uplift dome with a major axis oriented roughly southwest to northeast. The maximum uplift rate of more than 10 mm/yr is observed in the Gulf of Bothnia. The horizontal velocities are relatively low where the radial uplift rates are largest, and they are directed outward from this location on all sides, indicating a divergent motion of the crust. These rates increase with distance away from the uplift centre, and reach up to 2 mm/yr at sites far outside.

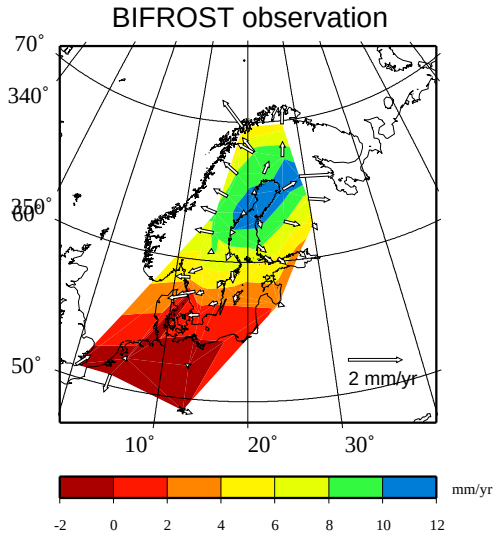

Figure 1.6: GPS observation of the crustal velocities (contours: vertical; arrows: horizontal) in Fennoscandia at BIFROST stations.

In this thesis both the RSL data [based on several studies and summarised in Lambeck, 1993a,b; Kaufmann and Wolf, 1996; Lambeck et al., 1998a; Vink et al., 2006] and the BIFROST results [Johansson et al., 2002] will be used.

1.1 Concept of the thesis

A number of factors, such as the ice-sheet geometry, the ocean load, the lithospheric thickness and the mantle viscosity affect the ongoing GIA. The most interesting factor is the mantle viscosity, as the time dependence of the GIA process is a characteristic of the viscosity. Thus, compared to the other factors only the mantle material produces significant GIA effects on the timescales of 10^4 to 10^5 years.

In general, the viscosity is a measure of the resistance of a fluid to deform under shear stress. It describes a fluid's internal resistance to flow and may be thought of as a measure of fluid friction. A typical example to visualise "What is viscosity?" is the comparison of water and oil: water is so-called "thin", having a lower viscosity, while oil is so-called "thick", having a higher viscosity.

The mantle viscosity was firstly introduced by Haskell [1935] in a hydrodynamic theory of postglacial rebound. He was able to determine a viscosity $\eta = 10^{21}$ Pa s of the upper mantle beneath Fennoscandia. In contrast, van Bemmelen and Berlage [1935] confined all mantle flow to a 100 km thick asthenosphere with a viscosity of $\eta = 1.3 \times 10^{19}$ Pa s, which should be the reason for the glacial rebound. Haskell instead found that by thickening their 100 km thick asthenosphere four times, the viscosity would agree with his one [Ekman, 1991]. This example demonstrates the difficulty in determining the mantle viscosity right from the start, and since then a large number of publications are dedicated to the GIA and the determination of the mantle viscosity, which will be extensively discussed in the following chapters.

The traditional theory of the GIA has been developed for a one-dimensional (1D) earth model [Peltier, 1974; Farrell and Clark, 1976; Milne and Mitrovica, 1998]. Several techniques can be used for the calculation, such as forward modelling using an iterative procedure in the spectral domain for predefined earth

Table 1.1: Summary of the numerical approaches used in the following chapters. The dimension of the investigated Earth structure is listed together with the source of the applied load and the number of the calculated models. The ice model FBKS8 is the Fennoscandian part of the global ice model RSES.

chapter	approach	dimension	load	model	model numbers
2	pseudo-spectral method	1D	ice/water	RSES	1089
	neighbourhood algorithm	1D	ice/water	RSES	1500
3	pseudo spectral method	1D	ice/water	RSES	1089
4	Finite-element method	3D	ice	FBKS8	10
5	Finite-element method	3D	ice	FBKS8	153
6	Finite-element method	1D	water	reservoir	3

models [pseudo-spectral approach after Mitrovica et al., 1994; Milne and Mitrovica, 1998], or inverse inferences [Tarantola and Valette, 1982; Mitrovica and Peltier, 1991]. The results of these modellings are compared to observational data such as the RSL data and the crustal velocities mentioned above. The numerical models of the GIA based on the Scandinavian and NW European observational data have converged towards a radial (1D) viscosity structure, with viscosities increasing by one to two orders of magnitude with depth. However, the mantle viscosity can vary in all three dimensions. Thus, in the GIA investigations the Finite-element (FE) technique is increasingly used in the last years. This method allows including lateral heterogeneities in the lithospheric thickness and in the mantle viscosity. Here, the application envelopes mixed spectral-FE codes [Martinec, 2000; Zhong et al., 2003], a finite volume formulation [Latychev et al., 2005b], and the use of commercial program packages [Wu, 2004; Spada et al., 2006].

In this thesis, we search for a consistent 3D viscosity structure of the Earth's mantle beneath Fennoscandia and NW Europe using both the forward and inverse modelling for 1D earth models and the FE method for 3D models. The forward and inverse techniques are used, as they are fast and efficient. The 1D-viscosity profiles found are used as input for the 3D investigations, which focus on different 3D viscosity structures and the sensitivity of the observational data to viscosity variations. Finally, the 3D modelling is used for a special investigation regarding the regional influence of a reservoir, again under the view of the Earth structure beneath and additionally in view of an influence on the instrument‘s registration in an observatory nearby. The 3D modellings are carried out with the commercial program package ABAQUS [Hibbitt et al., 2005].

Tab. 1.1 summarises all the numerical approaches used in this thesis, and lists the number of the calculated models and the sources of the applied load in each of the following chapters.

1.2 Outline of the thesis

This thesis consists of seven chapters. After this introduction five articles follow, with chapters 2, 4 and 6 already published in peer-reviewed journals and written by myself as first author. Chapter 3 is under revision at the moment and here I am a co-author. At the beginning of this chapter is stated for which sections I'm responsible. Chapter 5 is submitted to a peer-reviewed journal.

Chapter 2 discusses the topic of a weak asthenosphere underneath Fennoscandia and NW Europe. Therefore the pseudo-spectral approach and the Neighbourhood Algorithm (NA) are used. Earth models with

a special 1D structure are defined for the calculation. Then, the NA randomly creates additional earth models in a predefined range of lithospheric thickness and mantle viscosity. This allows us to explore the hypothesis of a low-viscosity zone in the upper mantle, which has been proposed in the literature. At first, a simple (three-layer) radial earth model is calculated for the subregions Scandinavia, NW Europe, and the Barents Sea, which best fits the sea-level data of those regions, then the global inverse procedure based on the NA is employed to further refine the viscosity profile in the upper mantle under the view of a possible asthenosphere. The global ice model RSES is used to predict the GIA of these earth models and the predictions are compared to the observed sea-level data from these regions and the BIFROST data. The results have been published in Steffen and Kaufmann [2005].

In chapter 3, the pseudo-spectral approach is used again to infer the radial Earth structure underneath the southern North Sea area. For this region, a comprehensive observational database of Holocene RSL index points from the NW European coast was recently compiled by the Bundesanstalt für Geowissenschaften und Rohstoffe (BGR). The data were collected from different countries / regions and by different workers. They were compared and reassessed by the BGR colleagues on a common time-depth scale. The database revealed a non-linear, glacio- and / or hydro-isostatic subsidence component, which is negligible on the Belgian coastal plain but increases significantly along the NW German coast. It was also found, that the subsidence is at least partly related to the post-glacial collapse of the so-called peripheral forebulge [see Kiden et al., 2002], which developed around the Fennoscandian ice-load centre during the last glacial maximum. Hence, special subsets of the new RSL data are compared to three-layer radial earth models as it is done in chapter 2. The aim is to infer the structure of the Earth mantle underneath the southern North Sea area, and conversely to predict RSL in regions of this area where no observational data are available. The results contribute to the investigations of Vink et al. [2006, submitted in July].

However, the former investigations only focus on a 1D Earth structure. The investigations in chapter 4 include the consideration of more complex earth models with lateral heterogeneities in the mantle viscosity. Here, a set of so-called flat 1D and 3D FE earth models with viscoelastic material properties is developed to study the GIA response induced by the ice-load model RSES. The emphasis is on a comparison of one 1D and three 3D viscosity models. The 1D viscosity model is a laterally homogeneous model based on the results of chapter 2, the 3D viscosity models are based on results of a shear-wave tomography. For the 3D structure, different rheological reference models were used. One aim is to investigate how the thermodynamic properties of the mantle affect the background radial viscosity profile and also the inferred lateral viscosity variations. Another aim is to study the different contribution of the lateral viscosity variations in various layers in the upper mantle and that from the lower mantle. In addition to the model comparison, a simple sensitivity analysis for different upper-mantle layers is performed to localise regions, which influence the rebound pattern. The GIA predictions of RSL change and crustal velocities are compared to observed sea-level data and the BIFROST project. The results of this chapter are published in Steffen et al. [2006a].

The results of chapter 4 put forward the question of the sensitivity of the present-day crustal velocities in Fennoscandia to radial and lateral viscosity changes in the upper mantle. Wu [2006] has recently shown such an analysis for the Laurentide Ice Sheet using an axially symmetric earth model with a simple symmetric ice model. His statistical approach is followed in chapter 5, but, (i) a *realistic* ice-load history of the Fennoscandian ice sheet (RSES ice model) is applied, and (ii) the *flat* 3D FE model from chapter 4 is employed. The model is subdivided into blocks of variable size, which results in a large number of sensitivity kernels to interpret. Thus, a simple approach is introduced to calculate the kernel of a block by averaging the perturbed predictions of all surface nodes of this block to one value for this block. The main emphasis is to show how sensitive BIFROST stations are to special mantle layers and regions and

to suggest locations for new GPS stations with higher sensitivity. The results of this chapter will be published in Steffen et al. [2006b, submitted in October].

In the chapters 4 and 5 the load is caused by ice. However, also water can be applied as load, as it is done in the first two chapters, where the sea-level equation is used and thus the mass imbalance of ice and water is calculated. In chapter 6, the load of the Hohenwarte reservoir in Thuringia, Germany, is used for the FE calculation. The calculated viscosity of chapter 2 is assigned in a FE model to investigate (i) if the reservoir load is large enough to deform the upper mantle, and (ii) the influence of lake-level fluctuations on regional deformation changes, which could possibly be observed with sensitive instruments in the nearby Geodynamic Observatory Moxa. It is focused on short-term elastic and long-term viscoelastic deformations resulting in tilt and strain. The results of this chapter are published in Steffen and Kaufmann [2006a,b].

Finally, chapter 7 concludes this thesis with a discussion of the results.